Polar Quasi-Confined Optical Phonon Modes in Wurtzite Quasi-One-Dimensional $GaN/Al_xGa_{1-x}N$ Quantum Well Wires*

Zhang Li†

(*Department of Mechanics and Electronics, Panyu Polytechnic, Panyu 511483, China*)

Abstract: Based on the dielectric continuum model and Loudon's uniaxial crystal model, quasi-confined (QC) optical phonon modes and electron-QC phonon coupling functions in quasi-one-dimensional (Q1D) wurtzite quantum well wires (QWWs) are deduced and analyzed. Numerical calculations on an AlN/GaN/AlN wurtzite QWW are performed. The results reveal that the dispersions of the QC modes are quite obvious only when the free wavenumber k_z in the z-direction and the azimuthal quantum number m are small. The reduced behavior of the QC modes in wurtzite quantum systems is clearly observed. Through the discussion of the electron-QC mode coupling functions, it is found that the lower-frequency QC modes in the high-frequency region play a more important role in the electron-QC phonon interactions. Moreover, our computations also prove that k_z and m have a similar influence on the electron-QC phonon coupling properties.

Key words: quasi-confined optical phonon modes; wurtzite quantum well wire; electron-phonon coupling
PACC: 7138; 6320K
CLC number: O471.3 **Document code**: A **Article ID**: 0253-4177(2006)10-1717-08

1 Introduction

High optical efficiency, strong atomic bonding, and wide band-gap are the typical characteristics of nitride semiconductor materials, which make the materials attractive as a basis for the creation of reliable high-temperature and high-frequency electronic equipments and short-wavelength optoelectronic devices[1~13]. For example, high-brightness blue/green nitride-based light-emitting diodes and lasers based on nitride quasi-two-dimensional planar heterostructures have been commercialized.

Recently, with the great progress of crystal growth technology, such as MBE, MOCVD, and HVPE, quasi-one-dimensional (Q1D) wurtzite GaN and ZnO quantum well wire (QWW) heterostructures have been successfully synthesized[2~4]. Q1D self-organized ZnO and GaN QWW ultraviolet lasers have a narrow emission linewidth and relatively low threshold[2,3]. It is well known that nanostructures provide important degrees of freedom for phonon engineering[14]. It may considerably change the density of phonon states, induce surface-related vibrations, and spatially confine the bulk phonon modes. Moreover, the Raman scattering spectra of Q1D wurtzite QWWs have also shown more complicated phonon vibration properties than those in zinc-blende planar and cylindrical heterostructures[5~7]. Due to the reduction of the dimensionality and the anisotropy of wurtzite structures, the properties of optical phonon modes in wurtzite QWWs have revealed more distinct phonon branches[8~13]. Therefore, it is important and necessary to investigate the lattice dynamic properties of wurtzite Q1D QWWs.

In fact, based on the dielectric continuum (DC) approximation and Loudon's uniaxial crystal model[15], several authors have made great contributions in studying polar optical phonons and their electron-phonon interactions in wurtzite nitride heterostructure systems[8~13]. For example, Gleize *et al*.[10] investigated the dispersion prop-

* Project supported by the Science and Technology Project of the Education Bureau of Guangzhou City (No. 2060) and the National Natural Science Foundation of China (No. 60390073)
† Corresponding author. Email: zhangli-gz@263.net
Received 6 February 2006, revised manuscript received 3 June 2006

erties of polar optical phonons in wurtzite GaN/AlN quantum wells and superlattices. Recently, Shi[11] exactly solved the equation of motion for the *p*-polarization field in an arbitrary wurtzite multilayer heterostructure by using the transfer matrix method. His results reveal that five types of optical phonons, including the quasi-confined (QC) modes, the interface optical (IO) modes, the propagating modes, the exactly confined modes, and the half-space (HS) modes, coexist in wurtzite multilayer quantum systems. On the basis of his work, Li *et al*.[12] further studied the dispersion properties of the QC optical phonon modes in multilayer GaN/AlN wurtzite QWs. In our recent work[13], the optical phonon modes in a cylindrical QWW were examined theoretically, and the existence of the QC phonon modes in the wurtzite QWWs was predicted. However, the properties of the QC modes in the wurtzite QWWs have not been fully understood. The purpose of this paper is to solve the QC phonon modes and derive the electron-QC phonon interaction Fröhlich-type Hamiltonian in a wurtzite Q1D heterostructure.

It is necessary to discuss the relationship between this work and that in our previous studies[17] in brief. In Ref. [17], with the matrix transfer method, the polar interface and surface optical phonon modes in a cubic multi-layer GaAs/AlGaAs Q1D quantum cable were investigated in detail. The frequency dispersion of the interface (surface) modes and electron-phonon coupling functions were numerically analyzed. The theoretical scheme in Ref. [17] can be looked at as a generalization of the interface optical phonon modes in general cubic-crystal Q1W QWWs with finite lay-number. Moreover, it was proved that there usually exist exact confined modes and interface modes, but there is no QC optical phonon mode in cubic-crystal quantum heterostructures in general. In the present research, the QC optical phonon modes in a wurtzite Q1D QWW with only two coaxial cylindrical heterostructures are deduced and studied. Hence the present work can be treated as an extensional attempt of confined phonon modes from cubic-crystal a Q1W quantum heterostructure to a wurtzite Q1W QWW system.

The main accomplishments and significance of this work are as follows. (1) Through the method of expanding the electrostatic potential, the free QC phonon field and corresponding Fröhlich electron-phonon interaction Hamiltonian in a wurtzite QWW have been derived. (2) The characteristics of the QC phonon dispersion and the electron-QC phonon coupling functions have been calculated and analyzed, and a detailed comparison of these characteristics with those in wurtzite planar heterostructure systems has been exhibited. (3) The present theoretical scheme and the numerical results are important and useful for further experimental and theoretical investigations of QC phonon effects in some complicated Q1D wurtzite heterostructures. In addition, in this paper, the QC phonon dispersion relations and the electron-QC phonon interaction Hamiltonian are deduced, and the numerical results for the dispersion of the QC optical phonon and the electron-QC phonon coupling functions for a GaN/$Al_xGa_{1-x}N$ QWW are reported and discussed.

2 Theory

Within the framework of the DC model, the electrostatic potentials $\Phi(\boldsymbol{r})$ of the polar vibrating modes in the wurtzite Q1D quantum well wires are determined by the second-order differential function

$$-\varepsilon_t(\omega)\nabla_t^2\Phi(\boldsymbol{r}) - \varepsilon_z(\omega)\nabla_z^2\Phi(\boldsymbol{r}) = 0 \qquad (1)$$

where ε_z and ε_t are the dielectric functions in the directions along and perpendicular to the *c*-axis of the wurtzite material, respectively. With the aid of Loudon's uniaxial crystal model[15], the electrostatic potential of the QC phonon modes (also the solutions of Eq. (1)) for an AlN/$Al_xGa_{1-x}N$/AlN wurtzite QWW can be written in cylindrical coordinates as

$$\Phi(r) = \sum_{m,k_z}\exp(\mathrm{i}m\varphi)\exp(\mathrm{i}k_z z)\begin{cases}A_1 I_m(\gamma_1 k_z\rho), & \rho \leqslant R_1\\ A_2 J_m(\gamma_2 k_z\rho) + B_2 Y_m(\gamma_2 k_z\rho), & R_1 < \rho \leqslant R_2\\ A_3 K_m(\gamma_3 k_z\rho), & \rho > R_2\end{cases} \qquad (2)$$

where m and k_z are the azimuthal quantum number and the free wave-number in the z-direction, respectively, $K_m(x)$ and $I_m(x)$ are the modified Bessel functions of the first and second kind, re-

spectively, and $J_m(x)$ and $Y_m(x)$ are the Bessel function and the Neumann function, respectively. $\gamma_i(i=1,2,3)$ is the ratio of the dielectric functions, defined by

$$\gamma_i(\omega) = |\zeta_i(\omega)|$$
$$\zeta_i = \mathrm{sign}[\varepsilon_{zi}(\omega)\varepsilon_{ti}(\omega)]\sqrt{|\varepsilon_{zi}(\omega)/\varepsilon_{ti}(\omega)|} \quad (3)$$

The QC phonon modes behave just like a confined electron in a quantum well with a finite potential barrier[8~12]. Hence the functions ζ_1 and ζ_3 should take positive values, and ζ_2 gets a negative value. Thus the QC modes display oscillating waves in the $Al_xGa_{1-x}N$ well materials and decaying waves in the AlN barrier materials[11~13].

Using the standard boundary conditions, i.e., the continuity of the phonon potential functions and their normal components of electric displacements at the interfaces $\rho=R_i(i=1,2)$, one can obtain the following formula in regard to the coupling coefficients A_i and B_i:

$$I_m(\gamma_1 k_z R_1)A_1 = J_m(\gamma_2 k_z R_1)A_2 + Y_m(\gamma_2 k_z R_1)B_2,$$
$$\varepsilon_{t1}\frac{\partial[I_m(\gamma_1 k_z\rho)]}{\partial\rho}\bigg|_{\rho=R_1}A_1 = \varepsilon_{t2}\frac{\partial[J_m(\gamma_2 k_z\rho)]}{\partial\rho}\bigg|_{\rho=R_1}A_2 + \varepsilon_{t2}\frac{\partial[Y_m(\gamma_2 k_z\rho)]}{\partial\rho}\bigg|_{\rho=R_1}B_2,$$
$$J_m(\gamma_2 k_z R_2)A_2 + Y_m(\gamma_2 k_z R_2)B_2 = K_m(\gamma_3 k_z R_2)A_3,$$
$$\varepsilon_{t2}\frac{\partial[J_m(\gamma_2 k_z\rho)]}{\partial\rho}\bigg|_{\rho=R_2}A_2 + \varepsilon_{t2}\frac{\partial[Y_m(\gamma_2 k_z\rho)]}{\partial\rho}\bigg|_{\rho=R_2}B_2 = \varepsilon_{t3}\frac{\partial[K_m(\gamma_1 k_z\rho)]}{\partial\rho}\bigg|_{\rho=R_2}A_3 \quad (4)$$

The condition that Eq. (4) has nontrivial solutions for A_i and B_i results in the following 4×4 determinant:

$$\begin{vmatrix} I_m(\gamma_1 k_z R_1) & -J_m(\gamma_2 k_z R_1) & -Y_m(\gamma_2 k_z R_1) & 0 \\ \varepsilon_{t1}\gamma_1[I_{m-1}(\gamma_1 k_z R_1) + I_{m+1}(\gamma_1 k_z R_1)] & -\varepsilon_{t2}\gamma_2[J_{m-1}(\gamma_2 k_z R_1) - J_{m+1}(\gamma_2 k_z R_1)] & -\varepsilon_{t2}\gamma_2[Y_{m-1}(\gamma_2 k_z R_1) - Y_{m+1}(\gamma_2 k_z R_1)] & 0 \\ 0 & J_m(\gamma_2 k_z R_2) & Y_m(\gamma_2 k_z R_2) & -K_m(\gamma_3 k_z R_2) \\ 0 & \varepsilon_{t2}\gamma_2[J_{m-1}(\gamma_2 k_z R_2) - J_{m+1}(\gamma_2 k_z R_2)] & \varepsilon_{t2}\gamma_2[Y_{m-1}(\gamma_2 k_z R_2) - Y_{m+1}(\gamma_2 k_z R_2)] & \varepsilon_{t3}\gamma_3[K_{m-1}(\gamma_3 k_z R_2) + K_{m+1}(\gamma_3 k_z R_2)] \end{vmatrix} = 0 \quad (5)$$

Equation (4) gives the dispersion relation of the QC optical phonon modes in a Q1D wurtzite QWW system.

Following the quantization steps for polar phonon fields as analogous to the interface optical phonons in wurtzite and cubic quantum systems[11~13,16,17], we get the free QC phonon fields as

$$H_{QC} = \sum_{m,k_z}\hbar\omega\left[b_m^{\dagger}(k_z)b_m(k_z) + \frac{1}{2}\right] \quad (6)$$

where $b_m^{\dagger}(k_z)$ and $b_m(k_z)$ are the creation and annihilation boson operators for phonons of the (m,k_z)-th modes, respectively. Moreover, the electron-QC phonon interaction Hamiltonian can also be obtained as

$$H_{e-QC} = -\sum_{m,k_z}\Gamma^{QC}_{m,k_z}(\rho)\times[\exp(im\varphi)\exp(ik_z z)b_m(k_z) + \mathrm{h.c.}] \quad (7)$$

where $\Gamma^{QC}_{m,k_z}(\rho)$ is the electron-phonon coupling function, defined as

$$\Gamma^{QC}_{m,k_z}(\rho) = N_{m,k_z}\times\begin{cases} g_1 I_m(\gamma_1 k_z\rho), & \rho\leqslant R_1 \\ g_2 J_m(\gamma_2 k_z\rho) + g_3 Y_m(\gamma_2 k_z\rho), & R_1<\rho\leqslant R_2 \\ g_4 K_m(\gamma_3 k_z\rho), & \rho>R_2 \end{cases} \quad (8)$$

In Eq. (8), N_{m,k_z} is the normalization constant, which is determined by the condition[18]

$$\frac{\hbar e^2}{2\omega} = \sum_{i=1}^{3}\frac{N^2_{m,k_z}\varepsilon_0}{2\omega}\int_{R_i}\mathrm{d}\boldsymbol{r}\left[\frac{\partial\varepsilon_{ti}(\omega)}{\partial\omega}\left|\frac{\partial\phi_i(\boldsymbol{r})}{\partial\rho}\right|^2 + \frac{\partial\varepsilon_{ti}(\omega)}{\rho\partial\omega}\left|\frac{\partial\phi_i(\boldsymbol{r})}{\partial\varphi}\right|^2 + \frac{\partial\varepsilon_{zi}(\omega)}{\partial\omega}\left|\frac{\partial\phi_i(\boldsymbol{r})}{\partial z}\right|^2\right] \quad (9)$$

The coupling coefficients $g_i(i=1,2,3,4)$ of the electrostatic potentials in Eq. (8), are defined as

$$g_1 = \varepsilon_{t2}\gamma_2 K_m(\gamma_3 k_z R_2)\{[J_{m-1}(\gamma_2 k_z R_1) - J_{m+1}(\gamma_2 k_z R_1)]Y_m(\gamma_2 k_z R_1) + J_m(\gamma_2 k_z R_1)[Y_{m-1}(\gamma_2 k_z R_1) - Y_{m+1}(\gamma_2 k_z R_1)]\} \quad (10)$$

$$g_2 = K_m(\gamma_3 k_z R_2)\{\varepsilon_{t1}\gamma_1 I_{m-1}(\gamma_1 k_z R_1)Y_m(\gamma_2 k_z R_1) + \varepsilon_{t1}\gamma_1 I_{m+1}(\gamma_1 k_z R_1)Y_m(\gamma_2 k_z R_1) + \varepsilon_{t2}\gamma_2 I_m(\gamma_1 k_z R_1)\times[Y_{m+1}(\gamma_2 k_z R_1) - Y_{m-1}(\gamma_2 k_z R_1)]\} \quad (11)$$

$$g_3 = -K_m(\gamma_3 k_z R_2)\{\varepsilon_{t1}\gamma_1 I_{m-1}(\gamma_1 k_z R_1)J_m(\gamma_2 k_z R_1) + \varepsilon_{t1}\gamma_1 I_{m+1}(\gamma_1 k_z R_1)J_m(\gamma_2 k_z R_1) + \varepsilon_{t2}\gamma_2 I_m(\gamma_1 k_z R_1)\times[J_{m+1}(\gamma_2 k_z R_1) - J_{m-1}(\gamma_2 k_z R_1)]\} \quad (12)$$

$$g_4 = \varepsilon_{t1}\gamma_1[I_m(\gamma_1 k_z R_1) + I_{m+1}(\gamma_1 k_z R_1)]\times[J_m(\gamma_2 k_z R_2)Y_m(\gamma_2 k_z R_1) - J_m(\gamma_2 k_z R_1)\times Y_m(\gamma_2 k_z R_2)] + \varepsilon_{t2}\gamma_2 I_m(\gamma_1 k_z R_1)\{[J_{m-1}(\gamma_2 k_z R_1) - J_{m+1}(\gamma_2 k_z R_1)]Y_m(\gamma_2 k_z R_2) + J_m(\gamma_2 k_z R_2)\times[Y_{m+1}(\gamma_2 k_z R_1) - Y_{m-1}(\gamma_2 k_z R_1)]\} \quad (13)$$

3 Results and discussion

In this section, we will further discuss the dispersive properties of QC modes and the coupling

behavior of electron-QC phonons. A wurtzite Q1D AlN/GaN/AlN QWW is chosen to perform numerical calculations. For convenience, the GaN well-material and AlN barrier-material will be denoted by subscripts 1 and 2, respectively. The widths of the QWW system are $2a_B/2a_B/\infty$ in Figs. 1 to 3 (a_B is the effective Bohr radius of the wurtzite GaN material, which is approximately 2.4nm). The material parameters used in our calculation come from Refs. [11~13].

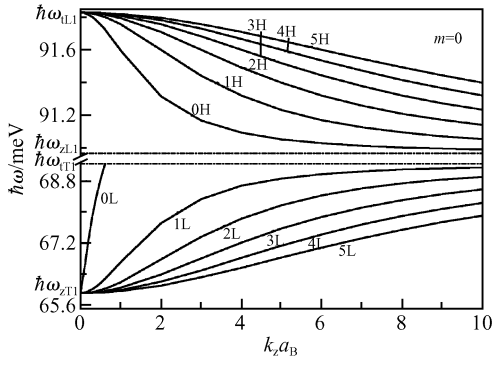

Fig. 1 Dispersion frequency $\hbar\omega$ of QC optical phonon modes as a function of the free wave-number k_z in the z-direction when the azimuthal quantum number m is kept at 0

The dispersion frequency $\hbar\omega$ of the QC optical phonon modes as a function of the free wave-number k_z in the z-direction is shown in Fig. 1. The azimuthal quantum number m is treated as a parameter and kept at 0 in the figure. From the figure, it can be seen that the frequencies of the QC modes fall into two independent frequency regions: the higher frequency region $\hbar\omega_{zL1} \sim \hbar\omega_{tL1}$ and the lower frequency region $\hbar\omega_{zT1} \sim \hbar\omega_{tT1}$. Thus the frequency ranges of the QC modes in the AlN/GaN heterostructures are completely determined by the characteristic frequencies of the GaN material[11]. The QC modes of higher frequency branches are labeled by iH, while those of lower frequency branches are denoted by iL. We can see that there are infinitely many branches of QC phonon modes for a given phonon wave-number k_z and azimuthal quantum number m, but only the first six branches are displayed in each range here. All of the QC modes in each region start from the frequency value $\hbar\omega_{zL1}$, $\hbar\omega_{tL1}$ for the low and high frequency regions, respectively, and go toward another frequency $\hbar\omega_{tT1}$, $\hbar\omega_{zL1}$ for the low and high frequency regions, respectively. The low-order modes (i.e. the modes iL and iH with little i) have stronger dispersion. For the same modes, the dispersion is strong at low and mediate wave-numbers k_z, and it becomes almost flat at larger k_z. Furthermore, all of the low-frequency modes are monotonic and incremental functions of the free wave-number k_z, while all of the high-frequency ones are monotonic and degressive functions of k_z. This feature is very different from the cases in wurtzite planar GaN/AlN quantum well systems[10,12]. In fact, the dispersion of low- (high-) frequency QC modes in single wurtzite quantum wells is a monotonic and degressive (incremental) function of k_z. The main reason for these distinctions is the different confined dimensionalities between quantum wells and quantum well wires[11~13].

It is worth mentioning that the 0L mode in the low-frequency region is special. The QC mode transforms to the interface modes after going beyond the frequency range of the QC mode. This is due to the overlap of characteristic frequencies between wurtzite GaN and AlN materials. Moreover, it also can be fully understood from the definition of $\gamma_i(\omega)$ in Eq. (3). Once $\omega > \omega_{tT1}$, the function $\gamma_1(\omega)$ becomes a positive value. The QC cannot exist in this situation, and it will decrease to become the interface optical modes[13].

Due to the Q1D confined properties of wurtzite quantum well wires, the dispersion frequencies of the QC modes are functions not only of k_z, but also of the azimuthal quantum number m. The QC mode frequencies $\hbar\omega$ of the first six branches in the low- and high- frequency regions as functions of m are plotted when k_z is kept at $5/a_B$ in Fig. 2. The frequencies are discrete functions of the quantum number m, and the broken lines in each curve are just guides for the eyes. Analogous to the case in Fig. 1, the dispersions are obvious only when m is small. The low-order QC modes with smaller i are more dispersive than the high-order ones with larger i. Each higher frequency branch (iH) is a monotonic and degressive function of m, while each lower frequency branch (iL) is a monotonic and incremental function of m, which is different from the dependence of $\hbar\omega$ on the wave-number k_z. The reduced behavior of the 0L mode is also clearly observed in Fig. 2, i.e., the 0L mode appears after the azimuthal

number m is over 1. The physical and mathematical reasons have been analyzed above.

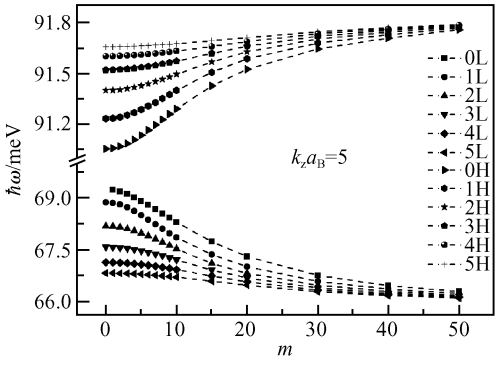

Fig. 2　QC mode frequencies $\hbar\omega$ of the first six branches in low- and high- frequency regions as functions of m when k_z is kept at $5/a_B$

Figure 3 depicts the electrostatic potential spatial distributions of the QC modes in the systems. The wave-number k_z and the azimuthal number m are parameters. For convenience, the coupling functions of the QC modes in the low frequency region (iL) have been enlarged 5, 10, and 100 times in Figs. 3(a), (b), and (c), respectively. For certain m and k_z, the electron-QC phonon coupling strengths for the higher frequency branches (iH) are far larger than those of the lower frequency branches (iL). Moreover, the low-order QC modes with smaller i relative to the high-order modes with bigger i play a more important role in the electron-phonon interaction. Comparing Figs. 3(a), (b), and (c), we find that the electron-phonon coupling magnitudes become weaker with the increasing of k_z and m. This reveals that the free wave-number k_z and the azimuthal quantum number m have similar influence on the electron-QC phonon coupling functions. Also the iH and iL modes only have $i-1$ node points in the well-layer region $R_1 \leqslant \rho \leqslant R_2$. This feature is quite analogous to the case of electronic states in finite quantum wells[10~12]. On the other hand, the electrostatic potential distributions of the QC modes in wurtzite QWWs are neither symmetric nor anti-symmetric, which is completely different from the situation in wurtzite planar quantum well heterostructures[12] due to the difference in their confined dimensionalities.

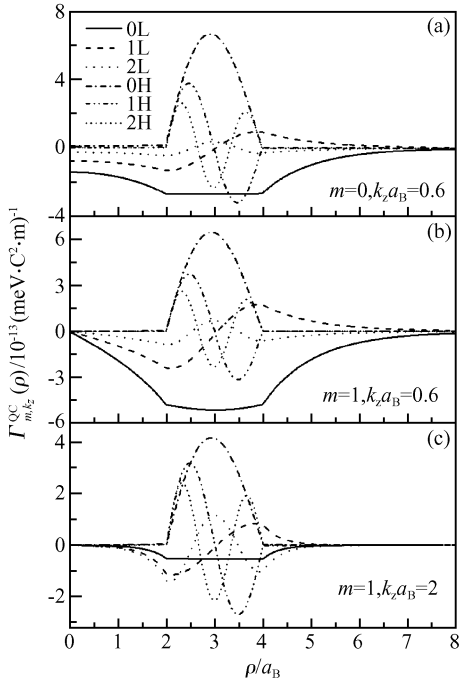

Fig. 3　Electron-QC phonon coupling functions $\Gamma^{QC}_{m,k_z}(\rho)$ as functions of ρ　The wave-number k_z and the azimuthal number m are kept at $k_z = 0.6/a_B$, $m = 0$ (a), $k_z = 0.6/a_B$, $m = 1$ (b), and $k_z = 2/a_B$, $m = 1$ (c), respectively.

In order to illustrate the influence of the well-width on the electron-QC coupling function, we plot $\Gamma^{QC}_{m,k_z}(\rho)$ in Fig. 4 as a function of ρ when wave-number k_z and the azimuthal number m are kept at 1. The parameters of the outer radius R_2 are chosen to be $3a_B$, $4a_B$, and $6a_B$ for Figs. 4(a), (b), and (c), respectively. The inner radius $R_1 = 2a_B$. The coupling functions of the low frequency branches (iL) in the figures have been enlarged 5 times for clarity. By comparing the figures, we find that except for the 0L branch, all of the other QC optical phonon modes increase obviously with the increase of the well-width ($R_2 - R_1$). For instance, as R_2 changes form $3a_B$ to $4a_B$, the peak value [in 10^{-13}(meV·C²·m)$^{-1}$] of the coupling function for the 0H branch increases from 4.77 to 5.89. Just like the analysis in Fig. 1, the behavior of the 0L branch is special. As the well-width of the wurtzite QWW becomes large, the electron-QC mode coupling strength of the 0L mode decreases noticeably. This discussion of the dependences of $\Gamma^{QC}_{m,k_z}(\rho)$ on the well-width reveals that for a wurtzite Q1D QWW with relatively larger well-width, more QC optical phonon branches must be included to satisfy the accuracy when the electron-QC interactions (such as the polaronic

effect and phonon scattering properties) are analyzed and calculated.

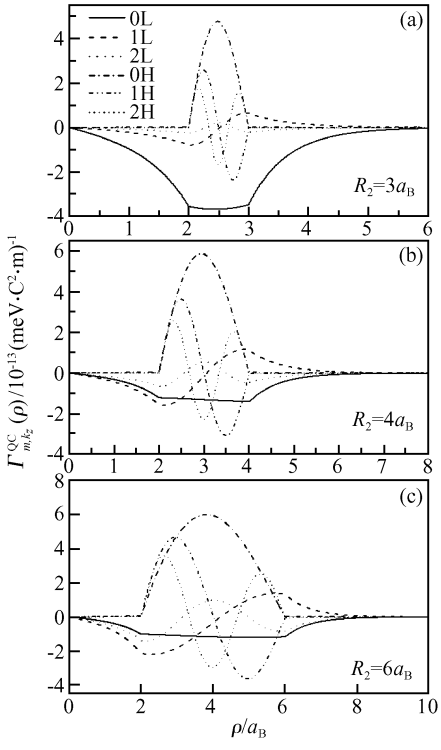

Fig. 4 $\Gamma^{QC}_{m,k_z}(\rho)$ as a function of ρ when $k_z=1/a_B$, $m=1$ for three different well-widths (a) a_B; (b) $2a_B$; (c) $4a_B$ The inner radius R_1 is kept at $2a_B$.

Finally, it is necessary to briefly discuss the influences of the cross-sectional shapes of the wurtzite Q1D QWWs and the material parameters constituting the QWW system. In this work, a cylindrical cross-section of the QWW is assumed for simplicity. In fact, the cross-sectional shapes of the QWW are affected by many complex factors, such as the material properties and the crystal growth conditions. Hence many Q1D QWWs with different cross-sectional shapes, such as cylindrical[2,4,5,16], rectangular[19,20], and triangular[21], have been reported and studied. Furthermore, different cross-sectional shapes of QWWs result in distinct optical phonon modes[22,23], a phenomenon which needs to be investigated and analyzed in detail. For example, there exist symmetric and antisymmetric interface modes in rectangular quantum wires[19,20], but the interface modes in cylindrical QWWs do not have this symmetry[16,17]. On the other hand, the material parameters constituting the Q1D heterostructure also greatly influence the characteristics of the optical phonon modes. Due to the anisotropy of wurtzite crystal, the characteristic frequencies of wurtzite materials are overlapping. Thus the frequency ranges of the QC modes may be completely different for different wurtzite heterostructures. For example, in an AlN/GaN/AlN heterostructure, the frequency ranges of the QC modes are $\omega_{zT,GaN}\sim\omega_{tT,GaN}$ and $\omega_{zL,GaN}\sim\omega_{tL,GaN}$, but the frequencies of the QC modes must fall into the ranges $\omega_{zT,GaN}\sim\omega_{tL,Al_{0.15}Ga_{0.85}N}$ and $\omega_{zL,GaN}\sim\omega_{tL,GaN}$ in an $Al_{0.15}Ga_{0.85}N/GaN/Al_{0.15}Ga_{0.85}N$ heterostructure[13]. Therefore, different materials not only change the parameters, but also influence the dispersion frequency ranges of the QC modes. Of course, the present theoretical schemes and formula of the QC phonon modes are effective and reliable for a general wurtzite Q1D heterostructure, and the different materials only affect the numerical results of the dispersions and the electrostatic potentials of the QC optical phonon modes.

4 Conclusion

In this paper, the QC optical phonon modes and Fröhlich electron-QC phonon interaction in wurtzite Q1D QWW systems were deduced and analyzed with the DC model and Loudon's uniaxial crystal model. The dispersion of the QC modes and the electrostatic potential distribution of a wurtzite AlN/GaN/AlN QWWs are calculated numerically. The results show that the dispersion of the QC modes sensitively depends on the free wave-number k_z and azimuthal quantum number m, especially when k_z and m are small. The reduced behavior of the QC modes in the wurtzite QWWs has been clearly observed, and reasonably physical and mathematical reasons have been analyzed. In the discussion of the electrostatic potential spatial distribution of the QC modes, it is found that the lower-order modes in the high frequency region make a more significant contribution to the electron-QC coupling interactions. The free wave-number k_z and azimuthal quantum number m have a similar influence on the electrostatic potential distribution of the QC modes. The well-width of the QWW also greatly affects the coupling strength of the electron-QC mode interaction. Furthermore, it is proved that the potential distribution of the QC modes is analogous to the electronic eigenstates in a finite quantum

well[10~13]. The present theories and numerical results are important and useful for further theoretical and experimental investigations of optical properties and the other effects and for device applications based on Q1D wurtzite quantum heterostructures.

Acknowledgement The author would like to acknowledge the detailed and valuable guidance and discussion of Prof. J. J. Shi of Peking University.

References

[1] Gil B. Group Ⅲ-nitride semiconductor compounds. Oxford: Clarendon Press, 1998
[2] Choi H J, Johnson J C, He R, et al. Self-organized GaN quantum wire UV laser. J Phys Chem B, 2003, 107: 8271
[3] Goldberger J, He R, Zhang Y, et al. Single-crystal gallium nitride nanotubes. Nature, 2003, 422: 599
[4] Zhang X H, Zhang Y, Song Y, et al. Optical properties of ZnS nanowires synthesized via simple physical evaporation. Physica E, 2005, 28: 1
[5] Liu H L, Chen C C, Chia C T, et al. Infrared and Raman-scattering studies in single-crystalline GaN nanowires. Chem Phys Lett, 2001, 345: 245
[6] Zhang J, Peng X S, Wang X F, et al. Micro-Raman investigation of GaN nanowires prepared by direct reaction Ga with NH_3. Chem Phys Lett, 2001, 345: 372
[7] Zhang J, Zhang L D. Morphology and Raman scattering spectrum of GaN nanowires embedded in nanochannels of template. J Phys D: Appl Phys, 2002, 35: 1481
[8] Lee B C, Kim K W, Stroscio M A, et al. Optical-phonon confinement and scattering in wurtzite heterostructures. Phys Rev B, 1998, 58: 4860
[9] Komirenko S M, Kim K W, Stroscio M A, et al. Dispersion of polar optical phonons in wurtzite quantum wells. Phys Rev B, 1999 59: 5013
[10] Gleize J, Renucci M A, Frandon J, et al. Anisotropy effects on polar optical phonons in wurtzite GaN/AlN superlattices. Phys Rev B, 1999, 60: 15985
[11] Shi J J. Interface optical-phonon modes and electron-interface-phonon interactions in wurtzite GaN/AlN quantum wells. Phys Rev B, 2003, 68: 165335
[12] Li L, Liu D, Shi J J. Electron quasi-confined-optical-phonon interactions in wurtzite GaN/AlN quantum wells. Eur Phys J B, 2005, 44: 401
[13] Zhang L, Shi J J, Tansley T L. Polar vibration spectra of interface optical phonons and electron-interface optical phonon interactions in a wurtzite GaN-AlN nanowire. Phys Rev B, 2005, 71: 245324
[14] Chen G, Zeng T, Borca-Tasciuc T, et al. Phonon engineering in nanostructures for solid-state energy conversion. Mater Sci Eng A, 2000, 292: 155
[15] Loudon R. The Raman effect in crystal. Adv Phys, 1964, 13: 423
[16] Xie H J, Chen C Y, Ma B K. Bound polaron in a cylindrical quantum wire of a polar crystal. Phys Rev B, 2000, 61: 4827
[17] Zhang L, Xie H J. Fröhlich electron-interface and -surface optical phonon interaction Hamiltonian in multilayer coaxial cylindrical $Al_xGa_{1-x}As$/GaAs quantum cables. J Phys: Condens Matter, 2003, 15: 5881
[18] Stroscio M A, Dutta M. Phonons in nanostructures. Cambridge: Cambridge University Press, 2001
[19] Stroscio M A. Interaction between longitudinal-optical-phonon modes of a rectangular quantum wire and charge carriers of a one-dimensional electron gas. Phys Rev B, 1989, 40: 6428
[20] Stroscio M A, Kim K W, Littlejohn M A, et al. Polarization eigenvectors of surface-optical phonon modes in a rectangular quantum wire. Phys Rev B, 1990, 42: 1488
[21] Sidor Y. Exciton in a quantum wire in the presence of parallel and perpendicular magnetic fields. Phys Rev B, 2005, 71: 165323
[22] Knipp P A, Reinecke T L. Classical interface modes of quantum dots. Phys Rev B, 1992, 46: 10310
[23] Chen C Y, Li W S, Yeung H K. Interface phonons in cylindrical GaAs/$Al_xGa_{1-x}As$ quantum dots. Solid State Commun, 1998, 106: 341

纤锌矿准一维 $GaN/Al_xGa_{1-x}N$ 量子阱线中的极化准受限光学声子模*

张 立†

（番禺职业技术学院机械与电子系，番禺 511483）

摘要：基于介电连续模型与 Loudon 的单轴晶体模型，推导分析了纤锌矿准一维量子阱线中的准受限(QC)光学声子模及相应的电子-QC 光学声子之间的相互作用函数.对一个 AlN/GaN/AlN 纤锌矿量子阱线进行了数值计算.结果显示，当体系的角量子数 m 与 z 方向上的自由波数 k_z 较小时，QC 光学声子模的色散相当明显.观察到纤锌矿量子体系中的 QC 光学声子模的“退化”行为.通过电子-QC 光学声子之间的耦合函数的讨论发现，高频区中的低频支 QC 模在电子-QC 光学声子模之间的相互作用中起主要作用.计算结果还证明自由波数 k_z 与角量子数 m 对电子-QC 光学声子模间的耦合特性具有相似的影响.

关键词：准受限光学声子模；纤锌矿量子阱线；电子-声子耦合

PACC：7138；6320K

中图分类号：O471.3 **文献标识码**：A **文章编号**：0253-4177(2006)10-1717-08

* 广州市教育局科技计划(批准号：2060)和国家自然科学基金(批准号：60390073)资助项目

† 通信作者. Email：zhangli-gz@263.net

2006-02-06 收到，2006-06-03 定稿